4 TAFLOVE, A.: 'Computational electrodynamics, the finite-difference time-domain method' (Artech House, Boston, 1995)
5 ESSELLE, K.P., OKONIEWSKI, M., and STUCHLY, M.A.: 'Analysis of sharp metal edges at 45 degrees to the FDTD grid', *IEEE Microw. Guid. Wave Lett.*, 1999, pp. 221–223
6 ESSELLE, K.P., and FOROUGHIPOUR, M.: 'Enhanced FDTD equations for sharp, diagonal, metal edges at arbitrary angles'. IEEE Antennas and Propagation Society (AP-S) Int. Symp., Atlanta, USA, June 1998, pp. 604–607
7 FOROUGHIPOUR, M., and ESSELLE, K.P.: 'Analysis of microstrip lines with diagonal edges using a singularity-enhanced FD-TD technique', *Microw. Opt. Technol. Lett.*, 1999, **23**, (2), pp. 121–123
8 ESSELLE, K.P., and FOROUGHIPOUR, M.: 'Analysis of an inclined microstrip patch antenna, using enhanced FDTD equations', *Electron. Lett.*, 1999, **35**, (11), pp. 853–854

Comparison of FDTD and SPICE simulations for lossy and dispersive nonlinear transmission lines

A. Jrad, W. Thiel, P. Ferrari and J.W. Tao

For the first time, a simulation has been carried out of lossy and dispersive nonlinear transmission lines (NLTLs) used for pulse compression, by two different time-domain approaches: SPICE and a full wave 3D finite difference time domain method. Results show good agreement between the two approaches. The output pulse risetime is strongly affected by DC and skin-effect losses.

Introduction: Nonlinear transmission lines (NLTLs) have been investigated for more than 30 years. More recently, Rodwell [1] demonstrated the ability of NLTLs to both generate shock waves with a subpicosecond fall time and to propagate ultrafast solitons. In the field of microwaves, when dealing with frequencies between a few gigahertz and a few hundreds of gigahertz, NLTLs are generally formed by coplanar waveguide (CPW) transmission lines with characteristic impedance Z_l, periodically loaded by reverse-biased Schottky contacts, which serve as voltage-variable capacitors.

The behaviour of NLTLs for pulse compression or harmonic generation is now well understood, but the simulation of lossy and dispersive CPWs used for NLTLs is still a problem. In [2], a simulation of microstrip NLTLs used for harmonic generation (with a sinusoidal excitation) by the harmonic balance method was presented. However, the harmonic balance method cannot be used for pulse compression where the excitation is a step-like waveform. In this Letter we present a comparison of two very versatile time-domain approaches: SPICE and the finite difference time domain (FDTD) method. The SPICE approach is described in [3, 4] for NLTLs. The 3D simulation was based on the standard FDTD method [5] also including transmission line losses.

To our knowledge, this is the first time that lossy and dispersive NLTLs have been simulated using the FDTD method with a full wave 3D approach. In [6], the FDTD method was applied to NLTLs and the results were compared to those obtained using SPICE. However, a lossless CPW was used, and a lumped-element model was implemented for the CPW in SPICE. It is clear that a distributed model must be implemented in SPICE because a lumped-element model fails when the frequency of the signal propagating along the NLTL reaches the Bragg frequency [1, 4].

NLTL basic principles: The NLTLs we consider in this Letter consisted of CPW transmission lines with characteristic impedance Z_l and propagation constant $\gamma = \alpha + j\beta$, periodically loaded by reverse-biased Schottky contacts, which serve as voltage-variable capacitors [1]. The CPW can be described by a distributed model as explained below (see Fig. 1). The diode is described by a series lumped-element model, with voltage-variable capacitance $C_d(V)$ and series resistance R_d. $C_d(V) = C_{j0}.f(V)$ where C_{j0} is the zero-biased diode capacitance value and the expression for $f(V)$ depends on the doping profile of the diode. In our case, a uniform doping profile was used; then $C(V) = C_{j0}\sqrt{(1+|V|/\phi)}$, where $\phi \simeq 0.7V$.

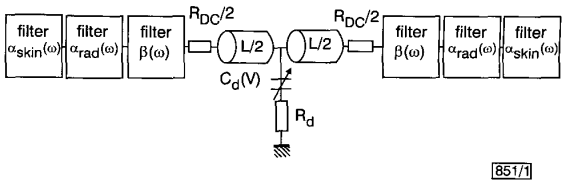

Fig. 1 *T-block for simulation of each section of NLTL in SPICE*

NLTL design: The NLTL was realised on an AsGa substrate. The method used for its design is described in [4]. It consisted of an NLTL with 100 elementary sections with a CPW characteristic impedance Z_l of 70Ω [7] and a zero-biased diode capacitance C_{j0} equal to 26fF. The large NLTL characteristic signal impedance was equal to 50Ω. The Bragg frequency was ~250GHz. The parameter values used for the CPW were: CPW ground plane width W_g = 60μm; CPW ground-signal separation S = 10.5μm; CPW centre conductor width W = 4.6μm; $\sigma = 37 \times 10^6$S/m; metal thickness t = 0.5μm; substrate thickness h = 200μm; ε_r = 13.1 (AsGa).

Simulation approaches:

(i) *FDTD:* In the 1D approach the coplanar line is approximated by a parallel plate waveguide resulting in a constant characteristic impedance and phase velocity. With this approach, only DC losses can be modelled. For modelling the attenuation of a transmission line in the 3D FDTD, a wideband approximation of metallic losses using the surface impedance approach based on a two-port model for the surface was included. A plane conducting sheet was assumed where the electric and magnetic fields on the top and the bottom side were described by an impedance matrix [8] derived from a plane-wave approach. This leads to a boundary condition for the magnetic field components surrounding the metal sheet. In both cases the diodes were incorporated into the FDTD method as lumped elements described in [9].

(ii) *SPICE:* Each NLTL section was simulated by the T-block shown in Fig. 1. The CPW transmission line was simulated by using the ideal transmission line model implemented in SPICE (L/2), a series resistance simulating R_{DC} (DC losses) and filters used to simulate skin-effect losses ($\alpha_{skin}(\omega)$), radiative losses ($\alpha_{rad}(\omega)$) and dispersion ($\beta(\omega)$). These filters were calculated by using the method described in [3, 4]. For calculating $\alpha_{skin}(\omega)$, skin-effect loss formulas developed by Heinrich were used (see [4]); for radiative losses and dispersion, we used Frankel's formulas (see [4]).

Simulation results: The input pulse generator $V_{in}(t)$ was a step-like waveform with V_h = 12 V, V_l = 0V and a risetime of 20ps.

(i) *CPW losses:* Before comparing the simulation results for NLTLs, we must verify that losses are correctly simulated by the two approaches, SPICE and FDTD. To achieve this, we considered only CPW transmission lines without diodes and compared the results obtained after simulation with Heinrich's formulas (see [4]).

For low losses, we can consider that the CPW is matched to the generator and load impedance. Then the CPW $S_{21}(\omega)$ parameter, calculated from FDTD and SPICE simulations, is equal to $\exp(-\alpha l)$. $S_{21}(\omega)$ is calculated as follows:

$$S_{21}(\omega) = FT[\text{output signal}(t)]/FT[\text{input signal}(t)]$$

where FT denotes Fourier transform. Results are shown in Fig. 2.

FDTD attenuation is greater up to 50GHz and smaller for higher frequencies. SPICE attenuation is lower than that of Heinrich's model above 20GHz. This is due to problems encountered for the simulation of R_{DC}. The deviation between Heinrich's formulas and the FDTD method are mainly based on the coarse grid which is used for the cross-section of the CPW.

(ii) *NLTL:* A comparison of the results from the SPICE and FDTD approaches is shown in Fig. 3. When only DC losses are considered, comparison between 1D FDTD and SPICE results shows good agreement (Fig. 3*a*). For the 3D FDTD method compared with SPICE for lossless CPW, the agreement is very good (Fig. 3*b*). This demonstrates the validity of the distributed CPW SPICE approach. When lossy CPWs are considered, we can see

that the agreement is acceptable if we consider risetimes, but we can note some differences in the magnitudes of the output pulses (Fig. 3*b*). These differences are related to low frequencies. We consider that this is mainly due to the differences in the simulation of the attenuation due to DC and skin-effect losses shown in Fig. 2.

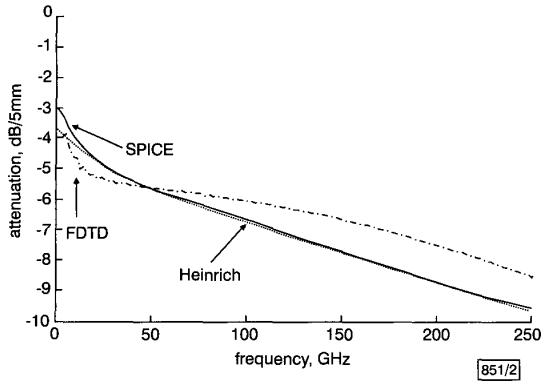

Fig. 2 *Attenuation obtained by FDTD and SPICE approaches for CPW (without diodes)*

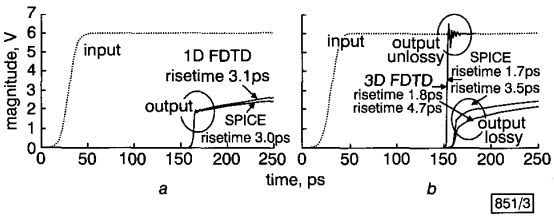

Fig. 3 *1D and 3D FDTD and SPICE simulation results when DC losses, lossless CPWs and all losses are considered*

a 1D FDTD and SPICE simulation results when only DC losses are considered
b 3D FDTD and SPICE simulation results when lossless CPWs are considered and when all losses (DC, skin-effect and radiation) and dispersion are considered

Conclusion: We have demonstrated SPICE and full wave FDTD simulations of lossy and dispersive NLTLs. The agreement between the two approaches is very good when considering the 1D FDTD method with CPWs DC losses or the 3D FDTD method with lossless CPWs. When we consider real CPWs, including DC, skin-effect, radiation losses and dispersion, the comparison shows a more severe attenuation for FDTD simulations. This difference seems to be related to differences in the attenuation obtained with the two approaches. Simulations also show the effect of CPW losses (mainly DC and skin-effect losses) on the output pulse risetimes (1.7ps without losses and > 3ps with losses) and magnitude (6V to ~2V).

14 March 2000
Electronics Letters Online No: 20000621
DOI: 10.1049/el:20000621

A. Jrad, P. Ferrari and J.W. Tao (*LAHC, Laboratoire d'Hyperfréquences et de Caractérisation, Université de Savoie, 73376 Le Bourget-du-lac Cedex, France*)

E-mail: ferrari@univ-savoie.fr

W. Thiel (*University of Ulm, Microwave Techniques, Albert-Einstein-Allee 41, 89069 Ulm, Germany*)

References

1 RODWELL, M.J.W.: 'Active and nonlinear propagation devices in ultrafast electronics and optoelectronics', *Proc. IEEE*, 1994, **82**, (7), pp. 1035–1059

2 SALAMEH, D., and LINTON, D.: 'Study of the effect of various parameters on nonlinear transmission-line (NLTL) performance', *IEEE Trans.*, 1999, **MTT-47**, (3), pp. 350–353

3 FERRARI, P.: 'Design and SPICE simulations of lossy and dispersive nonlinear transmission lines driven by a step-like generator', *submitted to IEEE Trans. Microw. Theory Tech.*, June 1999,

4 JRAD, A.: 'Study of NLTLs for the generation of ultra-short pulses'. PhD Thesis (in French), University of Savoy, 30 June 1999

5 YEE, K.: 'Numerical solution of initial boundary value problems involving Maxwell's equation in isotropic media', *IEEE Trans.*, 1966, **AP-14**, pp. 302–307

6 WANG, X., and HWU, J.: 'Theoretical analysis and FDTD simulation of GaAs nonlinear transmission lines', *IEEE Trans.*, 1999, **MTT-47**, (7), pp. 1083–1091

7 JRAD, A.: 'Choice of the CPW characteristic impedance for lossy nonlinear transmission lines synthesis', *Electron. Lett.*, 1999, **35**, (12), pp. 985–986

8 BOUZIDI, F.: 'Equivalent network representation of boundary conditions involving generalized trial quantities-application to lossy transmission lines with finite metallization thickness', *IEEE Trans.*, 1997, **MTT-45**, (6), pp. 869–876

9 PIKET-MAY, M., TAFLOVE, A., and BARON, J.: 'FD-TD modeling of digital signal propagation in 3D circuits with passive and active loads', *IEEE Trans.*, 1994, **MTT-42**, (8), pp. 1514–1523

Efficient calculation of far-field patterns of waveguide discontinuities using perfectly matched layers

H. Derudder, F. Olyslager and D. De Zutter

A new efficient method is outlined for calculating the far-field pattern of waveguide discontinuities. An open configuration is turned into a closed configuration using perfectly matched layers. Using a mode-matching scheme on the resulting configuration, the total field on the discontinuity can be determined. The far-field is calculated by taking the Fourier transform of this field and multiplying it by the Huygens' obliquity factor. Results are presented for a GaAs-AlGaAs laser facet and a truncated grounded dielectric slab.

Introduction: Slab waveguide structures are present in many photonic devices as well as in monolithic microwave integrated structures (MMICs) and printed circuit boards (PCBs). For semiconductor lasers a detailed knowledge of the far-field pattern is useful for properly utilising the emission in a particular application, e.g. the techniques for coupling the emission into an optical fibre and the resulting coupling efficiency depend on the far-field pattern of the heterostructure laser. On the other hand, the distributed and/or lumped elements in an MMIC interact through their interconnected ports (microstrips, striplines and via-holes). At high frequencies substrate waves can be induced which not only cause parasitic interactions between the components but can also give rise to external radiation at the side of the board by the scattering of the impinging substrate waves. Therefore, it is useful to have a calculation scheme which is able to calculate the far-field pattern of a substrate wave impinging on the end of a slab waveguide structure. In this Letter we propose such a method.

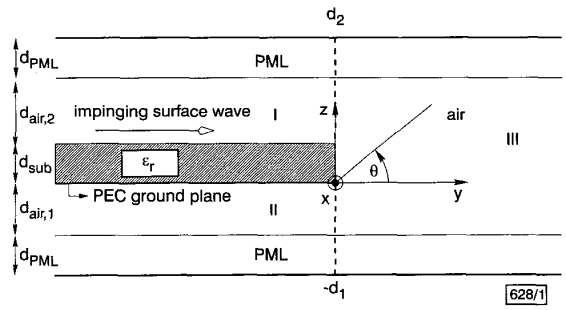

Fig. 1 *Truncated grounded dielectric slab with PMLs*
Structure is invariant in *x*-direction

Solution method: In the first step we enclose the original open structure by phase matched layers (PMLs) [1] backed with a